Nonsequential Double Ionization with Few-Cycle Laser Pulses

X. Liu
Max-Born-Institut, Max-Born-Strasse 2A, 12489 Berlin, Germany

C. Figueira de Morisson Faria
Institut für theoretische Physik, Universität Hannover, Appelstrasse 2, 30167 Hannover, Germany

(Received 23 October 2003; revised manuscript received 26 February 2004; published 2 April 2004)

We investigate differential electron momentum distributions in nonsequential double ionization with linearly polarized, few-cycle pulses, using a classical model based on a laser-assisted inelastic $(e^-, 2e^-)$ rescattering mechanism. These yields, as functions of the momentum components parallel to the laser polarization, are highly asymmetric and strongly influenced by the phase difference between the pulse envelope and its carrier oscillation, radically changing their sign around a critical phase. This behavior provides a powerful tool for absolute-phase measurements.

DOI: 10.1103/PhysRevLett.92.133006 PACS numbers: 32.80.Rm, 32.80.Qk

Recently, few-cycle laser pulses of intensities around or higher than 10^{14} W/cm^2 have proven to be extremely important. A particular characteristic of such pulses is that they may have very high intensities and, still, carry much less energy than their longer counterparts, such that, effectively, ionization is reduced. This has extended the damage threshold of solid-state materials up to the intensities in question [1], and has made the generation of high-order harmonic radiation up to astonishingly high frequencies possible [2]. Furthermore, their length, of the order of a few fs, permits controlling processes such as molecular motion or chemical reactions [3], as well as the production of isolated, x-ray attosecond pulses [4].

In this pulse-length regime, the so-called "absolute phase," i.e., the phase difference between the pulse envelope and its carrier frequency, radically influences strong-field phenomena, such as high-order harmonic generation (HHG) [2] and above-threshold ionization (ATI) [5,6]. Indeed, this phase determines, for instance, the maximal harmonic or photoelectron energies, the intensities in the spectra, and the time profiles of both phenomena.

This is not surprising, since the physics of HHG and ATI is directly related to the *instantaneous,* time dependent field. HHG, for instance, is described by a three-step mechanism in which an electron leaves an atom at an instant t_0 through tunneling ionization, propagates in the continuum under the influence of the external laser field, and, at a later time t_1, recombines with a bound state of the parent ion, generating harmonics [7]. Slightly different processes, either in which elastic rescattering with the parent ion is taken as the third step or in which the electron reaches the detector without recolliding explain the high-order and low-order ATI peaks, respectively [8].

In order to interpret the experimental data obtained in such cases, the precise knowledge of the absolute phase ϕ is required. This poses a serious practical problem, since this phase is difficult to stabilize, to control, or to measure [9]. For this reason, schemes for measuring ϕ have been suggested and realized, as, for instance, using the asymmetry in ATI photoelectron counts [6].

In this Letter, we propose laser-assisted nonsequential double ionization (NSDI) as a tool for absolute-phase diagnosis. This phenomenon is the subject of very active discussion, which was triggered by differential measurements of electron momentum distributions performed with the cold target recoil ion momentum spectroscopy technique, for linearly polarized fields of intensities of the order of $I \sim 10^{14}$–10^{15} W/cm^2 incident in rare-gas samples [10]. Such measurements revealed very peculiar features, namely, two symmetric peaks at $p_{1\|} = p_{2\|} = \pm 2\sqrt{U_p}$, in the $(p_{1\|}, p_{2\|})$ plane, where $p_{j\|}$ $(j = 1, 2)$ and U_p denote the momentum components parallel to the laser field polarization and the ponderomotive energy [11], respectively.

These features are explained by a physical mechanism very similar to those in HHG and high-order ATI. The main difference lies in the rescattering process at t_1, which is now inelastic: the first electron gives part of its kinetic energy upon return to the second electron, so that it can overcome the ionization potential of the singly ionized atom and reach the continuum [7]. This process has been considered by several groups, using classical [12], semiclassical [13,14], or quantum-mechanical [15,16] approaches, using different types of electron-electron interaction [13,14], and neglecting or including electron-electron repulsion in the final states [14,15]. So far, since the pulses involved were relatively long, they have been mostly approximated by monochromatic fields.

In particular, classical models reproduce the main features either observed experimentally or obtained by more refined, quantum-mechanical methods, astonishingly well. Indeed, recently, we have computed NSDI yields considering rescattering in its simplest form, i.e., electron-impact ionization, both classically and within a quantum-mechanical S-matrix framework, with practically identical results [14].

In this work, we use a similar classical model as in [14], in which an electron ensemble is subject to a few-cycle pulse $\mathbf{E}(t) = -d\mathbf{A}(t)/dt$, with the vector potential

$$\mathbf{A}(t) = A_0 \sin^2[\omega t/(2n)] \sin(\omega t + \phi)\hat{e}_x. \quad (1)$$

Thereby, ω, A_0, ϕ, and n denote the frequency, amplitude, absolute phase, and number of cycles, respectively. The electrons reach the continuum at a time t_0 with vanishing drift velocities and from the origin of the coordinate system. The start times are uniformly distributed, and the ejection probability per unit time, unless stated otherwise, is given by the quasistatic [17] tunneling rate

$$R(t_0) \sim \frac{1}{|E(t_0)|} \exp\left[\frac{-2(2|E_{01}|)^{3/2}}{3|E(t_0)|}\right], \quad (2)$$

where $|E_{01}|$ is the ionization potential of the atom in question. Subsequently, these electrons propagate under the influence of only the laser field. Finally, some of them return to the site of their release at $t_1 > t_0$ and free a second electron ensemble through inelastic collisions.

Each pair in such ensembles obeys

$$[\mathbf{k} + \mathbf{A}(t_0)]^2 = 0, \quad (3)$$

$$\int_{t_0}^{t_1} [\mathbf{k} + \mathbf{A}(t)]^2 dt = 0, \quad (4)$$

and

$$\sum_{j=1}^{2} [\mathbf{p}_j + \mathbf{A}(t_1)]^2 = [\mathbf{k} + \mathbf{A}(t_1)]^2 - 2|E_{02}|, \quad (5)$$

given in atomic units. Equation (3) expresses the energy conservation at the ionization time. Equation (4) imposes restrictions upon the intermediate electron momentum $\mathbf{k}$ such that the electron returns to its parent ion. Finally, Eq. (5) yields the energy conservation at the recollision time t_1. Thereby, the first electron gives part of its kinetic energy $E_{\mathrm{ret}}(t_1) = [\mathbf{k} + \mathbf{A}(t_1)]^2/2$ upon return to the second electron, so that it is able to overcome the ionization potential $|E_{02}|$ of the singly ionized atom. In terms of the momentum components parallel and perpendicular to the electric-field polarization, denoted $p_{j\parallel}$ and $\mathbf{p}_{j\perp}$ ($j = 1, 2$), respectively, Eq. (5) is written as

$$\sum_{j=1}^{2} [p_{j\parallel} + A(t_1)]^2 = [\mathbf{k} + \mathbf{A}(t_1)]^2 - 2|E_{02}| - \sum_{j=1}^{2} \mathbf{p}_{j\perp}^2. \quad (6)$$

For constant $\mathbf{p}_{j\perp}$, Eq. (6) describes a circle in the $(p_{1\parallel}, p_{2\parallel})$ plane, centered at $A(t_1)$ and whose radius depends on E_{ret}, $|E_{02}|$, and on $\mathbf{p}_{j\perp}^2$. Such momenta effectively shift the second ionization potential so that rescattering may become classically forbidden.

The electron momentum distributions then read

$$\Gamma \sim \int dt_0 \, R(t_0) \delta\left(E_{\mathrm{ret}}(t_1) - \sum_{j=1}^{2} \frac{[\mathbf{p}_j + \mathbf{A}(t_1)]^2}{2} - |E_{02}|\right), \quad (7)$$

where the argument of the δ function gives the energy conservation upon return and $\mathbf{p}_{j\perp}$ are integrated over. Details about this model are given in [14].

These distributions are displayed in the upper panels of Fig. 1, for neon [18], as density plots in the $(p_{1\parallel}, p_{2\parallel})$ plane. Their circular shapes and the maxima along $p_{1\parallel} = p_{2\parallel}$ are features also present for monochromatic driving fields [19], and mean, physically, that both electrons are leaving the parent ion most probably with equal parallel momenta. However, the fact that the yields are mainly concentrated in only one quadrant of the $(p_{1\parallel}, p_{2\parallel})$ plane makes them strikingly different from the former distributions, which are symmetric in $(p_{1\parallel}, p_{2\parallel}) \leftrightarrow (-p_{1\parallel}, -p_{2\parallel})$. Furthermore, around a critical phase ϕ_c [cf. Fig. 1(b)], the distributions start to change, until the whole yield is shifted from the first to the third quadrant. For increasing pulse length, these effects gradually disappear, so that the distributions become symmetric and phase-independent [Figs. 1(e)–1(h)].

Important questions concern the physical origin of both the asymmetry and the critical phase: are they caused by the phase space or by the tunneling rate (2)? Depending on the parameters, a whole phase-space region may become classically inaccessible, such that the radius of the circle described by Eq. (6) would collapse and the corresponding yields would vanish. The quasistatic tunneling rate, on the other hand, favors the start times t_0 for which the instantaneous field amplitude $|E(t_0)|$ is large, as compared to those for which $|E(t_0)|$ is small. Thus, the

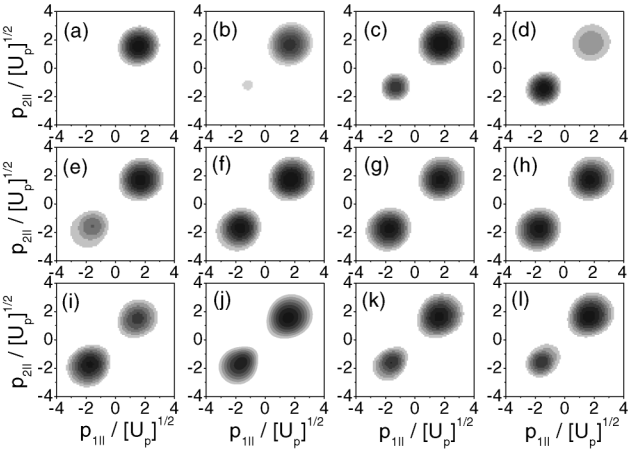

FIG. 1. Electron momentum distributions along the laser polarization, for neon ($|E_{01}| = 0.79$ a.u. and $|E_{02}| = 1.51$ a.u.), subject to pulses of intensity $I = 4.7 \times 10^{14}$ W/cm^2 and carrier frequency $\omega = 0.057$ a.u., respectively. In panels (a) to (d) and (i) to (l) we consider a four-cycle pulse ($n = 4$), whereas in panels (e) to (h) the pulse length is varied. Panels (a) to (h) and (i) to (l) were computed with the quasistatic and a constant tunneling rate, respectively. Panels (a) and (i) $\phi = 0.5\pi$; panels (b) and (j) $\phi = 0.8\pi$; panels (c) and (k) $\phi = 1.0\pi$; panels (d) and (l) $\phi = 1.2\pi$. Panels (e), (f), and (g) $n = 6$, 8, and 10, respectively, and $\phi = 0.5\pi$. In panel (h) n is the same as in (g) and $\phi = 1.2\pi$.

contributions from the former or from the latter case would be enhanced or suppressed, respectively. In order to single out the influence of the phase space, we assume that the electrons belonging to the first ensemble reach the continuum at a constant rate. Such results are shown in Figs. 1(i)–1(l) and are radically different from those obtained with the more realistic, quasistatic tunneling rate. Indeed, the momentum distributions, though asymmetric, exhibit peaks in *both* first and third quadrants of the $(p_{1\parallel}, p_{2\parallel})$ plane, vaguely resembling those obtained with monochromatic driving fields. The asymmetry is expected, since, for such pulses, the relation $A(t) = -A(t \pm T/2)$, and thus $|\Gamma(t_1, t_0, p_{1\parallel}, p_{2\parallel})| = |\Gamma(t_1 \pm T/2, t_0 \pm T/2, -p_{1\parallel}, -p_{2\parallel})|$, where $T = 2\pi/\omega$, which was true for monochromatic fields, no longer holds. However, the huge effects observed in the upper panels are absent. Physically, this means that there is a momentum region for which rescattering is classically allowed but for which the probability that the first electron reaches the continuum is very small. Consequently, even if this region is large, its contributions to the yield will be negligible.

In Fig. 2 we analyze this effect in detail. Therein, the electron start times t_0 are plotted, together with the quasistatic rate. We restrict the parameter range so that the classically allowed region is the largest [20], taking parallel momenta along the diagonal $p_{1\parallel} = p_{2\parallel} = p_\parallel$ and vanishing transverse momenta. We consider only pairs (t_0, t_1) of start and return times for the first electron such that its excursion time $\Delta t = t_1 - t_0$ in the continuum is of the order of $T/2$ [21]. For the specific parameters of the figure, there exist mainly two sets of electrons for which the quasistatic rate is large and, therefore, whose contributions are relevant: those ejected at $1.5T \lesssim t_0 \lesssim 2T$, with positive momenta, and those released at $2T \lesssim t_0 \lesssim 2.5T$, with negative momenta [22].

For a large range of absolute phases $\phi < \phi_c$, electron-impact ionization from the latter set of trajectories is classically forbidden, and the distributions concentrate on the first quadrant. Around the critical phase, this process is allowed for both sets of electrons and the tunneling rates are comparable. Consequently, there are relevant contributions to the yield in the first and third quadrants. For $\phi > \phi_c$, such as $\phi = 1.2\pi$, tunneling at $2T \lesssim t_0 \lesssim 2.5T$ is favored and $p_{j\parallel}$ are mainly negative.

The role of the phase space is even more evident as the driving-field intensity is varied, as shown in Fig. 3. By doing so, one is modifying the radius of the circle described by Eq. (6), and thus the region in the $(p_{1\parallel}, p_{2\parallel})$ plane for which rescattering is classically allowed. Hence, the critical phase may change. For a lower intensity than that in Fig. 1, the yield in the negative momentum region appears for a phase larger than $\phi_c = 0.8\pi$ [cf. Figs. 1(c) and 1(d)]. This is due to the fact that the classically allowed region for $p_\parallel < 0$ practically vanishes. Thus, even if the tunneling rates are comparable, the first electron, upon return, no longer possesses enough kinetic energy to release the second electron in a way that both leave with negative parallel momenta. For higher intensities, apart from the fact that both regions are classically allowed already below the expected ϕ_c, the high tunneling rates allow minor contributions also from $T < t_0 < 1.5T$. This is confirmed by Fig. 4, where, as the intensity decreases, the classically allowed region for the dominant set of ionization times ($2T < t_0 < 2.5T$), corresponding to $p_\parallel < 0$, collapses.

In conclusion, we perform a theoretical investigation of NSDI with few-cycle pulses, using a classical model based on electron-impact ionization. Both electrons have, most probably, equal final momentum components parallel to the field polarization which are mainly positive or negative. The sign of such momenta and their most probable value depend on the absolute phase ϕ. In particular, around a critical phase, this sign changes. Such features are explained as the interplay between the tunneling rate for the first electron and the phase space, and agree even quantitatively with quantum-mechanical computations [23].

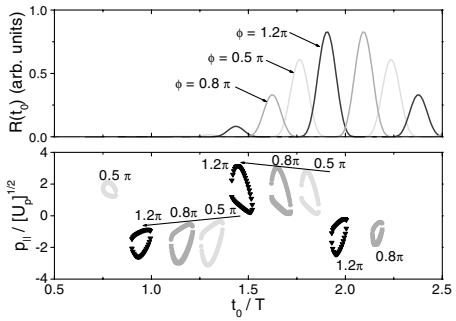

FIG. 2. Parallel electron momenta $p_\parallel$ along $p_{1\parallel} = p_{2\parallel}$, for $\mathbf{p}_{j\perp} = 0$ $(j = 1, 2)$, as functions of the start times t_0 of the electrons belonging to the first ensemble, in units of the field cycle, together with the quasistatic tunneling rates. The remaining parameters are the same as in Figs. 1(a)–1(d).

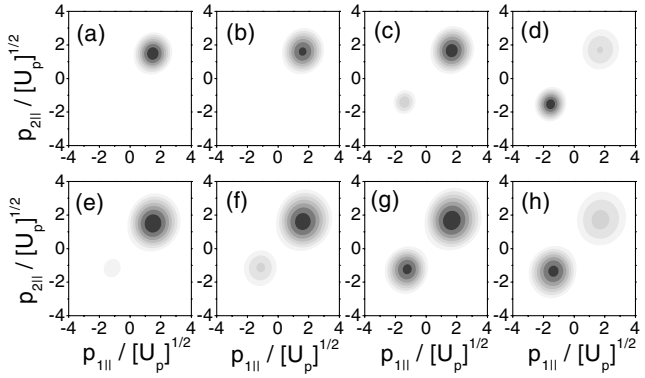

FIG. 3. Parallel electron momentum distributions for pulses of intensities $I = 4 \times 10^{14}$ W/cm^2 and $I = 8 \times 10^{14}$ W/cm^2 (upper and lower panels, respectively). The electrons were ejected with the quasistatic tunneling rate. The remaining parameters are the same as in Figs. 1(a)–1(d).

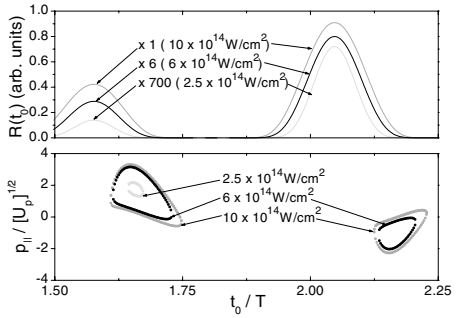

FIG. 4. Parallel electron momenta $p_{\parallel}$ along $p_{1\parallel} = p_{2\parallel}$ for $\mathbf{p}_{j\perp} = 0$ $(j = 1, 2)$, as functions of the start times t_0, together with the quasistatic tunneling rates, for several driving-field intensities and $\phi = 0.8\pi$. The remaining parameters are the same as in Fig. 3. For the lowest intensity, rescattering caused by electrons ejected at $2T < t_0 < 2.5T$ is classically forbidden, so that the corresponding curve is not displayed.

The modifications in the NSDI yields upon a critical phase are far more extreme effects than those observed for HHG or ATI. In fact, the advantage of NSDI over the other two phenomena is that it delimits a *confined* phase-space region. Thus, for particular ranges of ϕ, it is easier to make a whole region either classically forbidden, by causing the radius in Eq. (6) to collapse, or irrelevant, by reducing the corresponding tunneling rate. Hence, NSDI is a tool for absolute-phase diagnosis, which is, in principle, superior to the existing schemes.

We acknowledge W. Becker, A. Fring, and A. Sanpera for discussions and the Deutsche Forschungsgemeinschaft for financial support.

[1] M. Lenzner *et al.*, Phys. Rev. Lett. **80**, 4076 (1998).
[2] A. de Bohan, P. Antoine, D. B. Milošević, and B. Piraux, Phys. Rev. Lett. **81**, 1837 (1998); for a review cf. T. Brabec and F. Krausz, Rev. Mod. Phys. **72**, 545 (2000).
[3] M. Schnürer *et al.*, Phys. Rev. Lett. **85**, 3392 (2000); M. Hentschel *et al.*, Nature (London) **414**, 509 (2001); H. Niikura *et al.*, *ibid.* **417**, 917 (2002); A. Baltuska *et al.*, *ibid.* **421**, 611 (2003).
[4] M. Drescher *et al.*, Science **291**, 1923 (2001); P. M. Paul *et al.*, Science **292**, 1689 (2001); M. Kitzler *et al.*, Phys. Rev. Lett. **88**, 173904 (2002).
[5] In ATI, an atom absorbs more photons than is necessary for it to ionize, releasing high-energy electrons.
[6] P. Dietrich, F. Krausz, and P. B. Corkum, Opt. Lett. **25**, 16 (2000); G. G. Paulus *et al.*, Nature (London) **414**, 182 (2001); D. B. Milošević, G. G. Paulus, and W. Becker, Phys. Rev. Lett. **89**, 153001 (2002); Opt. Express **11**, 1418 (2003); S. Chelkowski and A. D. Bandrauk, Phys. Rev. A **65**, 061802(R) (2002).
[7] P. B. Corkum, Phys. Rev. Lett. **71**, 1994 (1993); M. Lewenstein *et al.*, Phys. Rev. A **49**, 2117 (1994).
[8] G. G. Paulus, W. Becker, W. Nicklich, and H. Walther, J. Phys. B **27**, L703 (1994).
[9] A. Apolonski *et al.*, Phys. Rev. Lett. **85**, 740 (2000); A. Baltuska *et al.*, *ibid.* **88**, 133901 (2002).
[10] R. Moshammer *et al.*, Phys. Rev. Lett. **84**, 447 (2000); B. Feuerstein *et al.*, *ibid.* **87**, 043003 (2001); T. Weber *et al.*, *ibid.* **84**, 443 (2000); Nature (London) **405**, 658 (2000).
[11] The ponderomotive energy is the temporal average $U_p = \langle A(t)^2 \rangle_t / 2$, where $A(t)$ is the vector potential. In order to compare our results more directly with the existing literature, we approximate it by the expression for the monochromatic case, i.e., $U_p = A_0^2/4$.
[12] J. Chen, J. Liu, L. B. Fu, and W. M. Zheng, Phys. Rev. A **63**, 011404(R) (2001); L. B. Fu, J. Liu, J. Chen, and S.-G. Chen, *ibid.* **63**, 043416 (2001); L. B. Fu, J. Liu, and S.-G. Chen, *ibid.* **65**, 021406 (R) (2002); J. Chen, J. Liu, and W. M. Zheng, *ibid.***66**, 043410 (2002); S. L. Haan, P. S. Wheeler, R. Panfili, and J. H. Eberly, *ibid.* **66**, 061402(R) (2002); R. Panfili, S. L. Haan, and J. H. Eberly, Phys. Rev. Lett. **89**, 113001 (2002).
[13] S. P. Goreslavskii, S. V. Popruzhenko, R. Kopold, and W. Becker, Phys. Rev. A **64**, 053402 (2001); S. V. Popruzhenko, Ph. A. Korneev, S. P. Goreslavskii, and W. Becker, Phys. Rev. Lett. **89**, 023001 (2002).
[14] C. Figueira de Morisson Faria, X. Liu, H. Schomerus, and W. Becker, Phys. Rev. A (to be published).
[15] A. Becker and F. H. M. Faisal, Phys. Rev. A **50**, 3256 (1994); M. Weckenbrock *et al.*, Phys. Rev. Lett. **91**, 123004 (2003).
[16] J. B. Watson *et al.*, Phys. Rev. Lett. **78**, 1884 (1997); D. Dundas, K. T. Taylor, J. S. Parker, and E. S. Smyth, J. Phys. B **32**, L231 (1999); W. C. Liu, J. H. Eberly, S. L. Haan, and R. Grobe, Phys. Rev. Lett. **83**, 520 (1999); C. Szymanowski *et al.*, Phys. Rev. A **61**, 055401 (2000); R. Kopold, W. Becker, H. Rottke, and W. Sandner, Phys. Rev. Lett. **85**, 3781 (2000); M. Lein, E. K. U. Gross, and V. Engel, *ibid.* **85**, 4707 (2000).
[17] L. V. Keldysh, Zh. Eksp. Teor. Fiz. **47**, 1945 (1964) [Sov. Phys. JETP **20**, 1307 (1965)].
[18] For neon, computations based on electron-impact ionization agree very well with the experiments. For other species, such as argon, excitation tunneling should also be considered [V. L. B. de Jesus *et al.* (unpublished)].
[19] This holds only if the interaction by which the first electrons dislodge the second is of contact type, i.e., $V_{12} = \delta(\mathbf{r}_1)\delta(\mathbf{r}_2 - \mathbf{r}_1)$. This interaction is implicit in Eq. (7). For other types of interactions see, e.g., Ref. [14].
[20] The start and return times coalesce at the maximal and minimal classically allowed momenta, defining a confined phase-space region. See, e.g., C. Figueira de Morisson Faria and W. Becker, Laser Phys. **13**, 1196 (2003).
[21] Longer excursion times are not relevant due to wave-packet spreading, which makes the overlap between the wave packets of the first and of the second electrons negligible. In our classical model, this implies leaving the corresponding electrons out of the ensemble.
[22] Other sets of electrons practically do not contribute to the yield, since the corresponding tunneling rate is very small. Their influence is seen if this rate is artificially taken to be constant (cf. lower panels of Fig. 1).
[23] C. Figueira de Morisson Faria *et al.* (to be published).